Thermochimica Acta, 196 (1992) 155–168
Elsevier Science Publishers B.V., Amsterdam

Ligational behaviour of ethyltrifluoroacetoacetate towards some tervalent lanthanons in aqueous–dioxane mixture

J.P. Shukla [a] and R.S. Sharma [b]

[a] *Radiochemistry Division, Bhabha Atomic Research Centre, Trombay, Bombay-400085 (India)*
[b] *Reactor Chemistry Section / RSMD, Bhabha Atomic Research Centre, Trombay, Bombay-400085 (India)*

(Received 7 June 1991)

Abstract

Thermodynamic step-wise formation constants ($\log {}^{T}K_n$) of some tervalent lanthanons, namely La, Pr, Nd, Sm, Eu, Gd, Dy, Er and Lu, with ethyltrifluoroacetoacetate, a fluorinated β-ketoester, have been determined pH-metrically in a 50 vol.% dioxane–water mixture at 25 and 35 ± 0.01°C. The method of Bjerrum and Calvin, as modified by Van Uitert and Haas, was used to calculate the formation functions $\bar{n}$ and free anion concentrations $[L^-]$. Thermodynamic formation constants, calculated on a high-speed computer following a weighted least-squares method, follow the order La < Pr < Nd < Sm < Eu $\geqslant$ Gd $\geqslant$ Dy < Er < Lu. Standard thermodynamic parameters $\Delta G^{\ominus}$, $\Delta H^{\ominus}$ and $\Delta S^{\ominus}$ associated with their first stepwise formation constant have also been evaluated. Speciation diagrams are depicted in three dimensions. An analysis of error is shown by plotting the weighted deviations against a tested variable. The choice of equilibrium model is justified by statistical analyses of S_{min} values, goodness-of-fit (GOF) and Abrahams–Keve-type normal probability plots.

INTRODUCTION

β-Diketones are well known chelating agents, capable of forming stable complexes with a host of cations. Tervalent lanthanon complexes of β-diketones have gained considerable importance owing to their varied practical applications in vapour phase chromatographic separations [1], solvent extraction of metals ions, as NMR shift reagents [2] and also as potential laser materials [3–5].

In general, lanthanons prefer ligands containing oxygen donor atoms such as β-diketones rather than nitrogen donors, and the coordination numbers are usually 8 or 9 [6]. It is surprising that the β-ketoesters which may also have similar applications, have not been explored extensively so far. Similarity in donor sites of β-ketoesters could provide some interesting comparisons with β-diketones. Scanty data are available on their complexation with bivalent metals and even less are available for complexation with

lanthanons. Mention may be made of the studies of Belfred et al. [7] on copper complexes of ethyltrifluoroacetoacetate and ethylacetoacetate (HEAA). Recently Dutt and Rahut [8,9] have prepared and made spectral studies of β-ketoesters with lanthanons.

A precise knowledge of the formation constants plays an important role in planning and selecting chelate processes for the separation of various metal components. No attempt seems to have been made to study the interaction of ethyltrifluoroacetoacetate (HETAA), a fluorinated β-ketoester, with tervalent lanthanons. Therefore, as a prelude to our studies on solid complexes of lanthanons with fluorinated β-ketoesters, thermodynamic formation constants (log ${}^{T}K_n$) of HETAA with tervalent lanthanons, namely La, Pr, Nd, Sm, Eu, Gd, Dy, Er and Lu, were determined pH-metrically in a 50 vol.% dioxane–water mixture at both 25 and 35 °C. The aquo–organic mixture had to be used because the ligand and its metal complexes are sparingly soluble in a pure aqueous medium.

EXPERIMENTAL

Reagent

A 10% aqueous solution of tetramethylammonium hydroxide (TMAH), G.R. grade, obtained from Merck, Germany, was diluted to 0.1 M in a 50% dioxane–water mixture and standardised against potassium hydrogen phthalate. The *p*-dioxane used was purified as recommended [10]. Perchlorates of lanthanons were prepared by dissolving AnalaR grade rare-earth oxides obtained from Alpha (Germany), were dissolved in perchloric acid. Metal perchlorates were standardised by ethylenediaminetetraacetic acid (EDTA) titration using xylenol orange as an indicator. HETAA was procured from Fairfield Chem. Co., USA, and used as received. All other chemicals were of A.R. or G.R. grade. Deionised water was used for preparing all solutions.

Apparatus

All pH measurements were made with a Beckman Research Model pH-meter, equipped with a glass combination electrode, which can be read to 0.002 pH units. It was standardised with phthalate and borax buffers before and after each titration. A water-jacketed titration vessel of nearly 80 ml capacity was used for all titrations. Electrode, burette and temperature probe were introduced in this vessel fitted with a Teflon stopper. The temperature of the reaction mixture was maintained constant by circulating water at the required temperature through the annular space between the walls. The reaction mixture was stirred with a magnetic stirrer.

Titration procedure

Titre solutions consisted of 0.01 M HETAA and 0.002 M tervalent metal perchlorate in appropriate dioxane–water solution to give 50% (v/v) final solvent composition. Due allowance for the contraction in volume on mixing 1:1 dioxane and water was made [11]. Whenever required, dilute perchloric acid was added to suppress initial complexation. The titration vessel with its contents was then thermostated at 25 and $35 \pm 0.1°$C. The titration was initiated by adding small aliquots of TMAH and noting the pH meter reading. Titrations were repeated until two sets of values differing by only ± 0.01 pH unit were obtained. For determining the thermodynamic dissociation constant ${}^{T}pK_a$ of the ligand, essentially the same procedure was followed, without addition of the metal ion solution.

CALCULATIONS

The hydrogen ion concentration $[H^+]$ of the solution was calculated from the pH meter reading (B) using the Van Uitert and Haas equation [12]

$$-\log[H^+] = B + \log U_H^{\ominus} - \log 1/\gamma \pm \quad (1)$$

The values of $\log U_H^{\ominus}$ were taken from the literature [11] and those of $\log 1/\gamma \pm$ were obtained by interpolating the data of Goldberg [13]. An extensive FORTRAN library TITRE was written on a NORSK-DATA computer at BARC which processes titration data for the computation of analytical concentrations, refinement of formation constants, data plotting and, finally, statistical assessment of the equilibrium model. Although basically similar in some respect to the procedure given by Schaefer [14], TITRE has some added features. The function minimised in our scheme is the weighted difference between observed $\bar{n}$ (average number of ligands bound per metal ion) and calculated $\bar{n}$. The parameter $\bar{n}$ was calculated at each point as follows

$$\bar{n} = ([TL] - [HL] - [L^-])/[TM] \quad (2)$$

where [TL], [HL], $[L^-]$ and [TM] denote the concentrations of total ligand, un-ionised ligand, free anion of the ligand and total metal, respectively. Our weighting scheme required a prior knowledge of an approximate estimate of the formation constants. The crude estimates of formation constants were obtained by putting unit weights to the experimental data for the first cycle of calculations. The weighted differences arising at this stage were those used at the end of a normal matrix build-up to determine the best set of parameters. The formation constants were refined by an iterative linear least-squares procedure.

Because determinations were not carried out at a fixed ionic strength of the medium, it was necessary to make corrections to the formation constants due to changes in the ionic strength. Therefore, values of ionic strength were calculated at each titration point. In the present study, total ionic strength, however, never exceeded 0.01 M.

Weighting scheme

The weighting scheme followed here takes into account the uncertainties in the values of pH and volume of alkali (V) added. If F is the weighted function minimised

$$F = \sum W(\bar{n}_{obs} - \bar{n}_{calc}) = \text{minimum}$$

for which the standard deviation σF is given as follows [14]

$$\sigma^2 F = [(\partial F/\partial[L])(\partial[L]/\partial pH) + (\partial F/\partial\bar{n})(\partial\bar{n}/\partial pH)]\sigma^2 pH + [(\partial F/\partial[L])(\partial[L]/\partial V) + (\partial F/\partial\bar{n})(\partial\bar{n}/\partial V)]\sigma^2 V \quad (3)$$

From propagation of error, the weight can now be defined as

$$W = 1/\sigma^2 F \quad (4)$$

Partial derivatives relating to the above were computed following the procedure described by Schaefer, except $\partial[L]/\partial V$ and $\partial\bar{n}/\partial V$ which were derived by cubic spline interpolation of $([L] - V)$ and $(\bar{n}, V)$ data [15] because no function relates them mathematically. Typically, $\sigma pH = 0.01$ pH unit and $\sigma V = 0.02$ ml, using the assumption that only random errors are present and thus that the goodness-of-fit (GOF) is unity. GOF can be defined as

$$GOF = \left\{\left[\sum(\Delta/\sigma)\right]/(N-n)\right\}^{1/2} \quad (5)$$

where Δ = deviation between observed and calculated values of $\bar{n}$, n = number of unknowns determined in a model, N = number of observations and σ = standard deviation of N values of Δ.

In terms of error analysis, TITRE follows the plot of residuals of pH and $\bar{n}$ against the observed values of pH and Abrahams–Keve-type normal probability plots (see Figs. 4 and 5, respectively, below) [16] for the assessment of the equilibrium model using pH data. This involved a comparison of the ordered distribution of experimental errors, $(\bar{n}_{obs} - \bar{n}_{calc})/\sigma\bar{n}$, with that expected from a normal distribution of the same sample size. An added feature includes the three-dimensional depiction of percentage distribution of the species present in the solution.

The stoichiometric step-wise formation constants K_n thus obtained were converted to thermodynamic constants ${}^{T}K_n$ incorporating the activity coefficient corrections as suggested in the literature [17].

RESULTS AND DISCUSSION

HETAA behaves as a weak monoprotic acid [18]. Values of ${}^{T}pK_a$ are found to be relatively lower when compared with that of HEAA, a non-fluorinated β-ketoester [19], in all proportions of dioxane and water. The data from a typical pH titration for evaluating the log ${}^{T}K_n$ values are given in Table 1 along with observed $\bar{n}$, weights, pL (negative logarithm of free anion concentration), and calculated values of pH and $\bar{n}$ obtained by substituting calculated molarity quotients in the equation

$$\bar{n} = \sum n\beta_n[L^-]^n / \left(1 + \sum \beta_n[L^-]^n\right) \tag{6}$$

A typical titration curve is shown in Fig. 1. Figure 2 depicts the experimental formation curve together with the calculated one. The formation curves did not show any dependence on varying metal concentration with fixed amount of the ligand, indicating the absence of any polynuclear species. A good overlap of the experimental and calculated formation curves justified the choice of the equilibrium model selected in all cases. A satisfactory model was obtained which consisted of ML_1, ML_2 and ML_3 complex species (charges are omitted for simplicity) with all the lanthanons. Generally, 4–5 iterations for refinements were sufficient for the final convergence of the models. It is evident from Table 2 that refinements usually converged at GOF values between 0.9 and 1.1 (the expected value being 1.0). We also tested the possibility of different models but the GOF showed a marked deviation from unity. The magnitude of the formation function $\bar{n}$ thus obtained was always higher (2.2–2.6) than the corresponding values (< 2.0) for Ln^{3+}–HEAA reported by Dutt and Rahut [20]. The absence of 1:3 complex species for HEAA with lanthanons cannot be simply attributed to steric factors alone as was suggested by the authors. Perhaps the basicity of the ligand and the different solvent medium used could be responsible for this unexpected behaviour.

Values of log ${}^{T}K_n$ are given in Table 2 along with corresponding $\bar{n}$ range, GOF, and the slope and intercept obtained from Abrahams–Keve-type plots. Values of S_{min} for lanthanon–HETAA complexes, which have the same statistical distribution as χ^2 with k degrees (number of unknowns) of freedom and with weights defined as above, are also recorded in Table 2. In particular, the log ${}^{T}K_1$ values steadily increase from La^{3+} to Eu^{3+} (Fig. 3) followed by a slight decrease up to Dy^{3+}, and then increasing again up to Lu^{3+}. However, an electrostatic interaction between the metal and ligand is evident for the lighter lanthanons. The behaviour observed here is not surprising; earlier studies with β-diketones also showed such a trend [21]. Similar irregularities have also been observed in some other notable properties of lanthanons, such as the Racaha parameters [22] and the standard entropies of the Ln^{3+}. Some authors have even tried to explain these effects using the so-called differential plots. This could,

TABLE 1

Typical titration data for lanthanon(III)–HETAA system in a 50 vol.% dioxane–water mixture at 25 °C [a]

Titrant (TMAH) (ml)	B pH meter reading	$\bar{n}$		pL	W (weights)	pH (Calc.)
		Obs.	Calc.			
0.26	3.260	0.030	0.017	7.211	0.427E−01	3.263
0.30	3.340	0.033	0.021	7.132	0.427E−01	3.343
0.34	3.430	0.040	0.025	7.043	0.430E−01	3.433
0.38	3.530	0.050	0.032	6.944	0.434E−01	3.533
0.42	3.674	0.057	0.044	6.801	0.432E−01	3.677
0.46	3.834	0.072	0.062	6.643	0.431E−01	3.837
0.52	4.060	0.110	0.101	6.421	0.435E−01	4.063
0.56	4.210	0.142	0.138	6.274	0.434E−01	4.213
0.60	4.332	0.178	0.177	6.155	0.434E−01	4.335
0.64	4.442	0.216	0.219	6.049	0.431E−01	4.446
0.68	4.540	0.255	0.263	5.955	0.425E−01	4.544
0.72	4.620	0.295	0.305	5.879	0.422E−01	4.624
0.78	4.726	0.356	0.367	5.779	0.416E−01	4.730
0.84	4.814	0.418	0.425	5.698	0.412E−01	4.818
0.90	4.912	0.480	0.497	5.606	0.387E−01	4.917
0.96	4.984	0.543	0.559	5.536	0.388E−01	4.985
1.02	5.054	0.606	0.620	5.473	0.372E−01	5.055
1.08	5.118	0.669	0.678	5.416	0.357E−01	5.118
1.14	5.182	0.732	0.741	5.359	0.335E−01	5.183
1.20	5.242	0.794	0.803	5.306	0.313E−01	5.243
1.30	5.332	0.899	0.900	5.228	0.283E−01	5.333
1.40	5.412	1.005	0.992	5.160	0.261E−01	5.412
1.50	5.496	1.110	1.095	5.088	0.226E−01	5.496
1.60	5.574	1.215	1.196	5.023	0.198E−01	5.574
1.70	5.646	1.320	1.296	4.961	0.178E−01	5.642
1.80	5.722	1.425	1.402	4.899	0.151E−01	5.718
1.90	5.800	1.530	1.515	4.835	0.124E−01	5.797
2.00	5.870	1.634	1.616	4.779	0.108E−01	5.866
2.10	5.948	1.739	1.731	4.716	0.868E−02	5.945
2.20	6.026	1.843	1.846	4.653	0.695E−02	6.024
2.30	6.104	1.947	1.957	4.591	0.562E−02	6.102
2.40	6.180	2.051	2.066	4.528	0.470E−02	6.175
2.50	6.260	2.155	2.165	4.468	0.395E−02	6.256
2.60	6.352	2.257	2.280	4.393	0.292E−02	6.349

[a] Titre volume, 50 ml; [HETAA], 0.010 M; [La^{3+}], 0.002 M; [TMAH], 0.106 M; [free $HClO_4$], 0.00955 M.

however, be summarised in the words of Wallace [23]: "if applied in general, the procedure will lead to the sought-for regularities where none exists". Irregularities in log ${}^{T}K_1$ versus $1/r$ can also be explained on the basis of the so-called 'tetrad effect". Great confusion still exists regarding the cause(s) of the tetrad phenomenon. Several attempts have been made

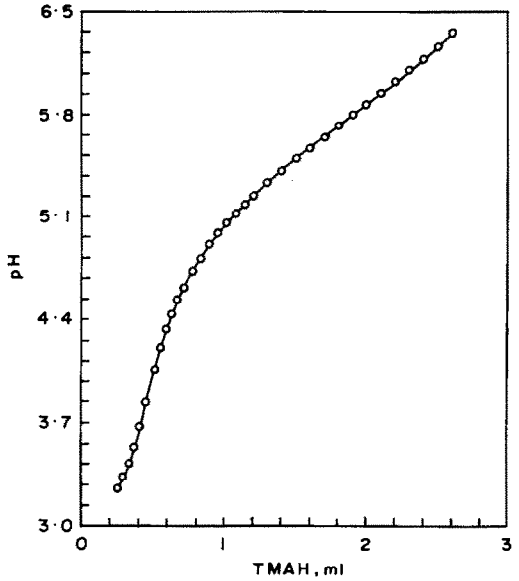

Fig. 1. Titration curve for La^{3+}–HETAA at 25 °C.

to theorise this effect which seek to propose its dependence on: discontinuity of the crystal radius of lanthanons [24]; change in coordination number of the metal cation [25]; change in hydration number [26]; and total angular

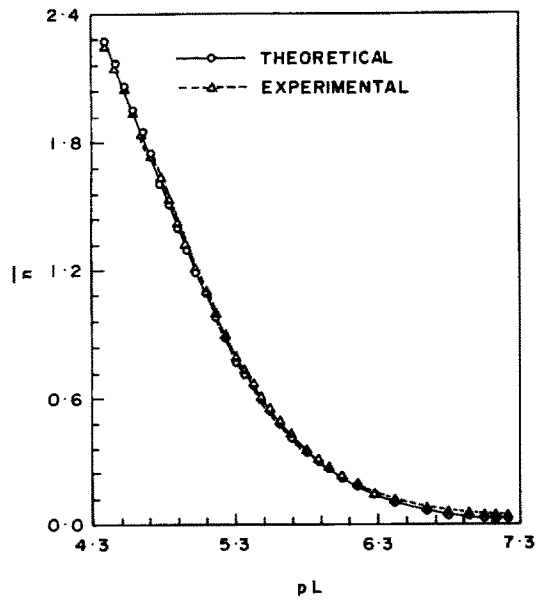

Fig. 2. Plot of calculated and observed $\bar{n}$ against pL for La^{3+}–HETAA at 25 °C.

TABLE 2

Thermodynamic step-wise formation constants of tervalent lanthanon complexes of HETAA in a 50 vol.% dioxane–water mixture

Metal ion	Temp (°C)	Weighted least-squares			$\bar{n}$ range	S_{min}	GOF	M [a]	C [a]
		$\log {}^{T}K_1$	$\log {}^{T}K_2$	$\log {}^{T}K_3$					
H^+	25	8.79±0.02							
	35	8.49±0.02							
La^{3+}	25	6.20±0.01	5.19±0.02	4.83±0.03	0.03–2.26	8.37×10^{-4}	1.03	0.99	0.12
($4f^0$)	35	6.06±0.01	5.21±0.01	4.64±0.01	0.03–2.64	4.11×10^{-3}	1.04	1.01	0.08
Pr^{3+}	25	6.55±0.01	5.43±0.01	5.09±0.01	0.02–2.45	4.75×10^{-3}	1.03	0.91	0.04
($4f^2$)	35	6.33±0.01	5.42±0.01	4.89±0.01	0.03–2.55	4.37×10^{-3}	1.04	1.00	0.09
Nd^{3+}	25	6.57±0.01	5.45±0.01	4.97±0.02	0.10–2.17	1.81×10^{-3}	1.03	0.99	−0.01
($4f^3$)	35	6.46±0.01	5.31±0.01	4.84±0.01	0.11–2.37	1.45×10^{-3}	1.03	0.85	−0.02
Sm^{3+}	25	6.66±0.01	5.75±0.02	5.13±0.02	0.04–2.14	2.02×10^{-3}	1.04	1.00	0.12
($4f^5$)	35	6.42±0.01	5.79±0.02	4.85±0.02	0.06–2.13	2.51×10^{-3}	1.03	1.00	0.05
Eu^{3+}	25	6.91±0.01	5.75±0.01	5.11±0.01	0.03–2.44	1.67×10^{-2}	1.03	1.02	0.02
($4f^6$)	35	6.52±0.01	5.65±0.01	4.82±0.01	0.05–2.65	2.60×10^{-2}	1.04	1.02	0.04
Gd^{3+}	25	6.90±0.01	5.71±0.02	5.26±0.02	0.03–2.45	1.11×10^{-2}	1.03	1.00	−0.02
($4f^7$)	35	6.52±0.01	5.67±0.01	5.13±0.01	0.04–2.73	4.05×10^{-3}	1.03	1.01	−0.04
Dy^{3+}	25	6.81±0.01	5.89±0.01	4.62±0.01	0.08–2.22	1.78×10^{-3}	1.03	1.01	0.04
($4f^9$)	35	6.93±0.01	5.89±0.02	4.62±0.02	0.13–2.34	3.19×10^{-2}	1.02	0.91	0.28
Er^{3+}	25	6.91±0.01	5.92±0.01	4.57±0.01	0.04–2.18	3.05×10^{-3}	1.04	1.01	−0.02
($4f^{11}$)	35	6.99±0.01	5.95±0.01	4.67±0.01	0.06–2.36	1.55×10^{-2}	1.02	0.99	0.10
Lu^{3+}	25	6.99±0.01	5.88±0.02	4.74±0.03	0.14–2.30	7.97×10^{-3}	1.03	1.01	−0.00
($4f^{14}$)	35	7.06±0.01	5.98±0.01	4.82±0.01	0.07–2.33	1.09×10^{-2}	1.02	0.99	0.06

[a] Slope (M) and intercept (C) are calculated from normal probability curves of Abrahams–Keve plots [16].

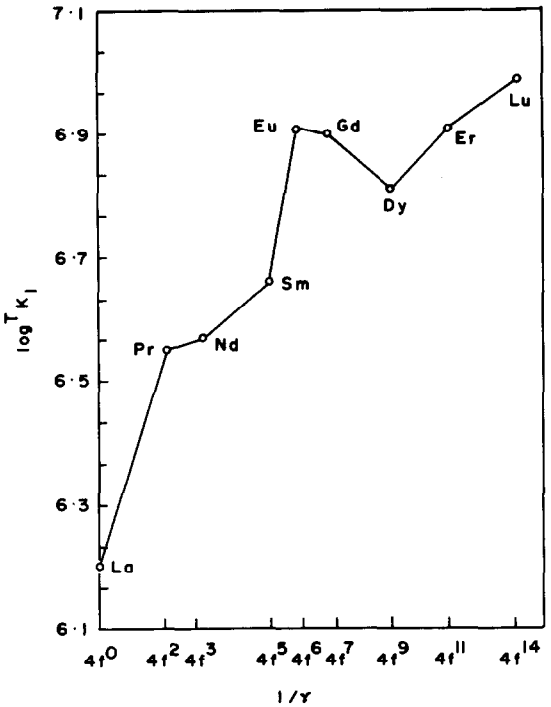

Fig. 3. Plot of log $^{T}K_1$ vs. $1/r$ for Ln^{3+}–HETAA at 25 °C.

momentum L of the lanthanons [27], the "inclined W" hypothesis. None of these explanations, however, seems to be fully acceptable [28].

Analysis of error

The absolute values of least-squares residuals $(pH_{obs} - pH_{calc})/\sigma pH$ $(= \delta)$ and $(\bar{n}_{obs} - \bar{n}_{calc})/\sigma\bar{n}$ served as statistics for the analysis of variance. TITRE is coded to test the dependence of δ on pH and volume of alkali. Figure 4 gives the distribution of δ(pH and $\bar{n}$) as a function of pH (experimental) and shows the effect of the weighting scheme. The weighted deviations δ approximate a random distribution as a function of pH, which is a tested variable for this effect. Figure 5 shows an Abrahams–Keve-type normal probability plot of the ordered weighted differences as a function of expected probability from a Gaussian distribution of random errors of the same sample size. The observed distribution is nearly symmetrical about the zero value and the slope of the curve is almost unity, as expected if only random errors were present in an experiment. This leads to the conclusion that our weighting scheme can properly estimate the true random errors and no systematic experimental errors were present. An improper selection of the model also gives rise to systematic errors in calculations. Our choice of model selection appears to be appropriate in the present study.

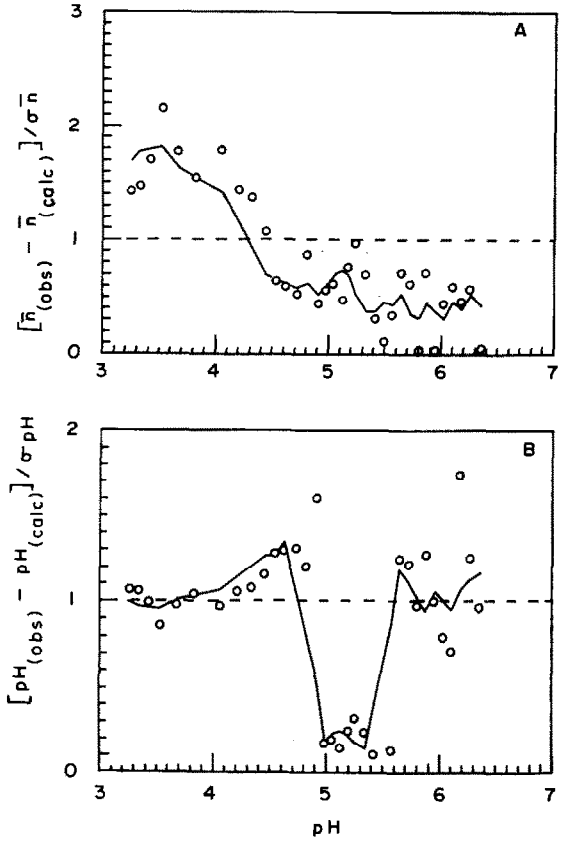

Fig. 4. Plot of pH and $\bar{n}$ residuals for La^{3+}–HETAA at 25 °C.

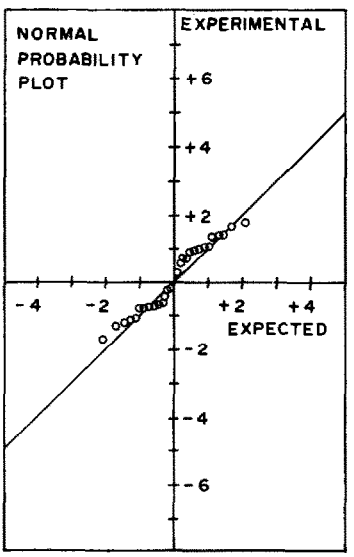

Fig. 5. Normal probability curve for La^{3+}–HETAA at 25 °C.

Thermodynamic functions

Table 3 records the values of thermodynamic functions calculated for $\log {}^{T}K_1$ only. Standard thermodynamic parameters for chelation were calculated following the equations

$$\Delta G^{\ominus} = -2.303RT \log {}^{T}K_1$$

$$\Delta H^{\ominus} = 176.06(\log {}^{T}K_1^{308.2} - \log {}^{T}K_1^{298.2})$$

$$T\Delta S^{\ominus} = \Delta H^{\ominus} - \Delta G^{\ominus}$$

The $\Delta G^{\ominus}$ values reported here may be lacking in accuracy, because several factors influence the stability of the complex. Nevertheless, a qualitative prediction concerning the nature of the complexation could easily be arrived at within the limits of the experimental errors. Large negative values of $\Delta G^{\ominus}$ obtained for Ln(III)–HETAA complex indicate the spontaneity of the complexation reactions. Furthermore, because the ionic potential increases from La^{3+} to Lu^{3+}, $\Delta G^{\ominus}$ values became more negative, thereby proving the predominant electrostatic interaction between Ln^{3+} and HETAA which is in conformity with our conclusion. Values of $\Delta H^{\ominus}$ for Ln^{3+}–HETAA chelates are negative up to Gd^{3+} and then become positive, at least from Dy^{3+} to Lu^{3+}. Owing to small differences between values of stability constants at the two temperatures, the entropy values showed a fluctuation. Apart from a few cases, complex formation seemed to be favoured by only the entropy term, countermanding the unfavourable enthalpy factor. Large positive values of $\Delta S^{\ominus}$ in a few systems with significant differences in $\log {}^{T}K_1$ values at the two temperatures, showed an enhancement in the entropy of the system. This increase could be due to the large number of water molecules released from the inner coordination sphere of the metal as a result of the bidentate nature of the β-ketoester ligand.

Speciation

The speciation of HETAA–Ln(III) chelates was determined by calculating percentage formation of all the species at each point of titration using β_n values calculated from the respective experiments. The percentage distribution of various complex species as a function of pH and pL was drawn by TITRE on a high-speed Calcomp Plotter. Figure 6 depicts the speciation of HETAA–La(III) chelate in three dimensions. For clarity, all the species are plotted separately. As the pH or free anion concentration increased, free metal ion gradually diminished and complexation progressively took place in a step-wise manner. For example, the percentage formation of M^{3+}, being about 99% at pH 3.26, was drastically reduced to 27% as the pH was raised to 5.41, whereas the formations of ML_1^{2+}, ML_2^{+}

TABLE 3

Thermodynamic parameters $\Delta G^{\ominus}$, $\Delta H^{\ominus}$, $\Delta S^{\ominus}$ calculated from the formation of first step-wise ($\log {}^{T}K_1$) Ln^{3+}–HETAA complexes [a]

Function	Temp. (°C)	La ($4f^0$)	Pr ($4f^2$)	Nd ($4f^3$)	Sm ($4f^5$)	Eu ($4f^6$)	Gd ($4f^7$)	Dy ($4f^9$)	Er ($4f^{11}$)	Lu ($4f^{14}$)
$\log {}^{T}K_1$	25	6.20	6.55	6.57	6.66	6.91	6.90	6.81	6.91	6.99
	35	6.06	6.33	6.46	6.42	6.52	6.52	6.93	6.99	7.06
$-\Delta G^{\ominus}$	25	35.37	37.38	38.05	38.51	38.05	38.34	38.55	38.90	39.90
	35	35.50	37.34	38.13	37.88	38.51	38.47	40.90	41.27	41.69
$\Delta H^{\ominus}$		−23.78	−38.39	−19.55	−42.28	−33.28	−40.65	21.31	13.90	13.19
$T\Delta S^{\ominus}$	25	11.59	–	17.96	–	–	–	60.19	53.37	53.08
	35	11.73	–	18.61	–	–	–	62.20	55.17	54.88

[a] Thermodynamic parameters ($\Delta G^{\ominus}$, $\Delta H^{\ominus}$, $T\Delta S^{\ominus}$) are expressed in kJ mol^{-1}.

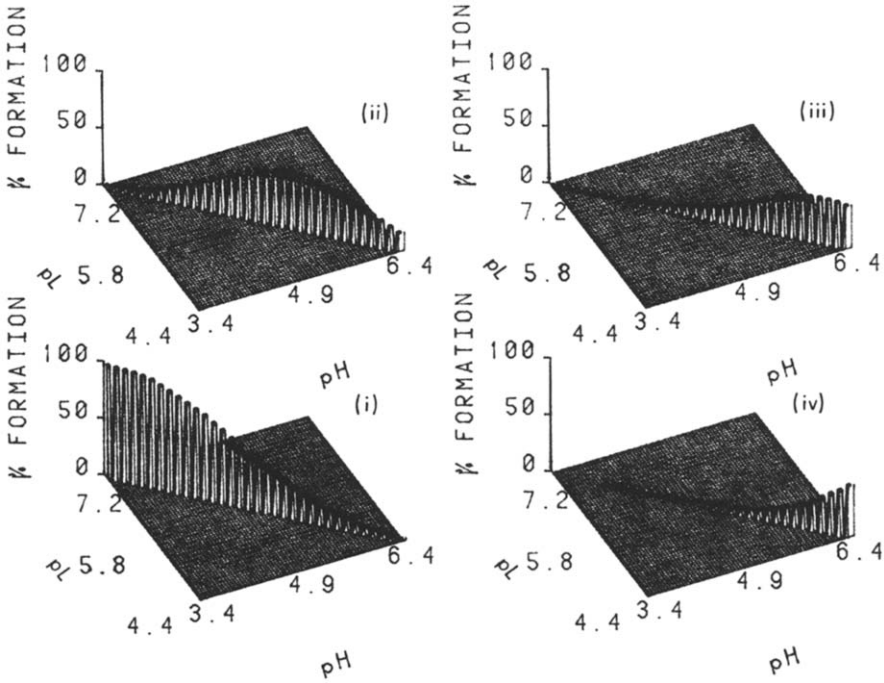

Fig. 6. Speciation diagrams (i) La^{3+}, (ii) $La(ETAA)_1^{2+}$, (iii) $La(ETAA)_2^{+}$ and (iv) $La(ETAA)_3$ (temp. 25 °C).

and ML_3 complexes were around 50%, 19% and 4% respectively at the same pH (Fig. 6).

ACKNOWLEDGEMENTS

The authors thank Dr. P.R. Natarajan, Head, Radiochemistry Division and Dr. L.H. Prabhu, Head, Reactor Chemistry Section, RSMD/ROMG for their keen interest in this work.

REFERENCES

1 N. Ahmed, N.S. Bhacca, J. Serbin and J.W. Wander, J. Am. Chem. Soc., 93 (1971) 2564.
2 R.E. Rodeau and R.E. Sievers, J. Am. Chem. Soc., 93 (1971) 1522.
3 H. Samelson and A. Lempicki, J. Chem. Phys., 39 (1963) 110.
4 R.G. Charles and E.P. Riedel, J. Inorg. Nucl. Chem., 28 (1966) 3005.
5 A. Lempicki and H. Samelson, Phys. Lett., 4 (1963) 133.
6 T. Moeller, in J.C. Bailer, H.J. Emeleus, R. Nyholm and A.F. Trotman Dickenson (Eds.), Comprehensive Inorganic Chemistry, Vol. 4, Pergamon, New York, 1973, pp. 24, 25.
7 R.L. Belfred, A.E. Martell and M. Calvin, J. Inorg. Nucl. Chem., 17 (1964) 759.
8 N.K. Dutt and S. Rahut, J. Inorg. Nucl. Chem., 32 (1970) 2909.
9 N.K. Dutt and S. Rahut, J. Inorg. Nucl. Chem. , 33 (1971) 1725.

10 A. Weissberger and E.S. Proskauer, Organic Solvents, Vol. 7, Interscience, New York, 1955, p. 139.
11 J.P. Shukla and S.G. Tandon, J. Electroanal. Chem., 35 (1972) 423.
12 L.G. Van Uitert and C.G. Haas, J. Am. Chem. Soc., 75 (1953) 451.
13 D.E. Goldberg, J. Chem. Educ., 7 (1963) 341.
14 W.P. Schaefer, Inorg. Chem., 4 (1965) 642.
15 C. deBoor, A Practical Guide to Splines, Springer–Verlag, New York, 1978, Chapt. 14.
16 S.C. Abrahams and E.T. Keve, Acta Crystallogr. Sec. A, 27 (1971) 157.
17 B. Rao and H.B. Mathur, J. Inorg. Nucl. Chem., 33 (1971) 2919.
18 J.P. Shukla and R.S. Sharma, J. Prakit. Chem., 332 (1990) 619.
19 N.S. Al-Niami and B.M. Al-Saadi, J. Inorg. Nucl. Chem., 35 (1973) 4207.
20 N.K. Dutt and S. Rahut, J. Inorg. Nucl. Chem., 31 (1969) 3177.
21 B.A. El-Shetary, S.L. Stefan, M.S. Abdel-Moez and M.M. Mashalay, Can. J. Chem., 66 (1988) 2362.
22 S. Verma and M.C. Saxena, J. Indian Chem. Soc., 64 (1987) 725.
23 R.M. Wallace, Inorg. Nucl. Chem. Lett., 7 (1971) 305.
24 S.K. Gray, S. Mukherjee, B.S. Garg and R.P. Singh, J. Indian Chem. Soc., 59 (1982) 1038.
25 E.J. Wheelwright, F.H. Spedding and G. Schwarzenbach, J. Am. Chem. Soc., 75 (1953) 4196.
26 G.R. Choppin and A.J. Graffeo, Inorg. Chem., 4 (1965) 1254.
27 S.P. Sinha, Helv. Chim. Acta, 58 (1978) 7.
28 R.J.P. Williams, Struct. Bonding (Berlin), 50 (1982) 81.